Chaotic Quantum-inspired Evolutionary Algorithm: enhancing feature selection in BCI

Alimed Celecia Ramos
Electrical Engineering Department
PUC-Rio
Rio de Janeiro, Brazil
alimedcr22@gmail.com

Marley Vellasco
Electrical Engineering Department
PUC-Rio
Rio de Janeiro, Brazil
marley@ele.puc-rio.br

***Abstract*—Quantum-inspired Evolutionary Algorithms (QiEAs) have demonstrated to be very effective in several applications. In particular, employing this algorithm for feature selection as a wrapper technique in Brain-Computer Interfaces applications was recently proposed with great results. Moreover, the training time of the model was decreased while maintaining a high classification accuracy, both essential conditions for a successful BCI. The drawback of this model was the sensitiveness to changes in the direction and magnitude of the rotation angle, which can produce adverse effects in both performance and convergence time. Chaotic systems and Evolutionary algorithms, when combined, can enhance the convergence rate and speed of the evolutionary process, incrementing the capacity of reaching the global optima. In this paper we explore the effects of adding ergodicity to a QiEA by the employment of chaotic maps in two operators: chaotic uniform crossover and chaotic quantum update gate. To validate the proposed approach, six commonly used chaotic maps are tested with data of Motor Imagery (MI) Electroencephalography (EEG) of right and left hand movement. The results of these experiments are compared with the ones of a QiEA and a classical Genetic Algorithm (GA). In the proposed model, Wavelet Packet Decomposition is employed as the time-frequency analysis to characterize the signal, whereas a Multilayer Perceptron Neural Network is used as a classifier. The results demonstrated that Chaotic QiEAs can significantly improve the convergence time of the model with only a small loss in the final accuracy.**

Keywords—Feature selection, Chaotic maps, Quantum-inspired Evolutionary Algorithm, BCI applications, Motor Imagery classification

I. INTRODUCTION

The translation of scientific theories that explain natural phenomena into Computational Intelligence algorithms is a core paradigm in this field of knowledge. One of the most promising examples of this is the combination of Quantum Computing and Evolutionary Computing [1], [2]. Applications of these algorithms range from engineering optimization problems [3] and healthcare [4], to feature selection [5] and neural architecture search [6]. These approaches are defined as Quantum-inspired Evolutionary Methods, and integrate Quantum Computing elements as Quantum Bits (Qubits), Quantum Gates, coherence, and entanglement, to produce highly efficient algorithms.

The main advantages of this category of algorithms are the great balance between exploitation and exploration, the capacity of finding a global solution with a small number of individuals [7], and the fast convergence [8]. Nevertheless, these models present a high sensitivity to the selection of the direction and magnitude of the rotated angle [5], [8], which affects directly their convergence capacity and time.

A novel approach to enhance the convergence rate and speed of evolutionary algorithms, as well as their capacity to reach the global optima is to incorporate a component of chaotic behavior through ergodic chaotic signals. Such a method is successfully combined with algorithms as Differential Evolution [9], Particle Swarm Optimization [10], or Genetic Algorithms (GA) [11]. However, this approach is rarely applied with Quantum-inspired Evolutionary Algorithms, even with evidence that qubits have chaotic characteristics [12]. In [12], chaos updating quantum gate is proposed to increment the efficiency of the evolutionary algorithm with good results in both convergence capacity and temporal complexity. Reference [13] introduced a real-coded quantum-inspired evolutionary algorithm that included a chaotic mutation operator for Fuzzy Neural Networks (FNN) training. The results of the simulation demonstrated the speed of convergence of the model to an optimal FNN. The work described in [14] added a chaos interference operator to a quantum-inspired evolutionary algorithm for grey image thresholding, outperforming the classical counterpart algorithm (GA). Employing chaotic maps, in [15] variants of chaotic crossover, quantum gates, and control of population dynamics were implemented. The resultant performances for several benchmarks validated the superiority of a quantum-inspired evolutionary algorithm that combines the approaches mentioned.

A valuable application for these enhanced Quantum-inspired Evolutionary Algorithms (QiEAs) are the processing stage of Brain Computer Interfaces (BCI). These neuro-technology devices have as objective the translation of brain signals in communication commands for any external tool. Commonly, in noninvasive BCI, the brain activity produced by predefined mental or physical tasks are measured through electroencephalography (EEG), following by a complex processing procedure that intents to identify which task produced such signals [16]. The task recognition is based on

This work was sponsored by CNPq and FAPERJ Brazilian Agencies.

978-1-7281-6929-3/20/$31.00 ©2020 IEEE

the application of Computational Intelligence algorithms related to feature computation, selection and classification.

BCI systems demand high performance and faster convergence given that, for each user, it is needed to train the whole signal processing pipeline. Moreover, EEG signals present really challenging conditions, being characterized by nonlinearities, small amplitudes, poor spatial resolution, high sensitivity to artifacts, and pronounced variations in time. Therefore, the search for a robust processing pipeline that is both fast and highly accurate is extremely relevant for the application of BCI devices.

Recently, we proposed a QiEA that improved the feature selection stage of Motor Imagery (MI) EEG data for Brain Computer Interfaces (BCI) [5]. The results obtained with three different subjects for the model in a wrapper approach with binary representation and a Multilayer Perceptron Neural Network (MLP) to classify right- and left-hand movements indicated the superiority of this method over a classical GA. Nonetheless, it was highlighted the great influence of the magnitude of the rotated angle in both convergence speed and performance of the QiEA.

In this work, our objective is to explore the capacity of adding ergodicity to a QiEA through the utilization of different chaotic maps [17] to produce a chaotic crossover operator and chaotic quantum update gate. Moreover, the algorithm will be applied for the feature selection task as a wrapper approach in MI EEG signals classification, which, to the extent of our knowledge, is not reported in the literature. The proposed Chaotic Quantum-inspired Evolutionary Algorithm (CQiEA) is evaluated by comparing the classification performance of an MLP obtained from three subjects available from BCI Competitions II and III with a classical GA (best method from [18]) and the QiEA proposed in [5].

The remainder of the paper is organized as follows: next section offers a detailed description of the methods utilized in each of the signal processing stages (Preprocessing, Feature Extraction, Feature Selection, and Classification), offering more attention to Chaotic Systems and QiEAs. Section III presents the datasets employed and the results obtained for the different evolutionary models, discussing their significance. Lastly, Section IV provides the final remarks of our work.

II. Materials and Methods

As stated in [5] and [19], our proposed BCI system comprises four stages (Fig. 1) for the analysis of EEG signals. The following sections describe the methods employed for each stage, dedicating more time to the Feature Selection and QiEAs in particular.

A. Preprocessing and Feature Extraction

EEG signals present significant randomness, extreme variations in time, and non-stationarity. These characteristics establish, as objectives in a Preprocessing stage, the removal of muscular or Electrooculography artifacts and other unwanted components existing in the signal, and the improvement of the Signal to Noise Ratio (SNR) [20]. Additionally, the signals are prepared for the feature extraction stage by the application of some temporal or spectral analysis.

In our application, we apply a time-frequency analysis that not only allows representing the signal in both temporal and spectral domains through meaningful features but also separates the components of the signal in different informative frequency sub-bands. The selected method was the Wavelet Packet Decomposition (WPD), which is recommended for non-stationary, random, and transient signals [21].

The WPD is an extension of the Discrete Wavelet Transform (DWT) that employs a consecutive set of high and low band filters to decompose the signal into shifted and scaled versions of a waveform known as mother wavelet. This multistep approach offers a hierarchical structure in which the components of different frequency sub-bands are represented by wavelet coefficients. For a detailed explanation of the algorithm please refer to our previous work [18].

To apply this model, it was chosen the mother wavelet Daubechies of order 4 (db4) and four decomposition levels. As a result, the signal is decomposed (in the last level) into sixteen sub-bands with a bandwidth of 4Hz, from which eight sub-bands are selected to represent the MI EEG signal: 0-4Hz, 4-8Hz, 8-12Hz, 12-16Hz, 16-20Hz, 20-24Hz, 24-28Hz and 28-32Hz. These sub-bands were selected following evidence presented on the literature [22], [23] that a broad spectrum band - including delta (from 0.5 to 4Hz), theta (4-7Hz), and gamma (30-40Hz) - can improve the accuracy of the analysis and classification of MI BCI applications.

Fig. 1. Stages of the proposed BCI system.

After obtaining the different sub-bands, for each of them the signal is reconstructed (an example of the results for one EEG channel can be observed in Fig. 2). Then, the signal of each sub-band is described by a combination of statistical, power and phase descriptors. Those selected features are commonly used separately for EEG signals processing, with the exception of the energy ratio of adjacent sub-bands, which was proposed by the authors based on another work that employed the ratio of other metrics [24]. The final feature vector comprises 134 features, as Table I illustrates.

B. Feature Selection

Due to the high dimensionality of the feature vector and looking for a subset of features that could improve both the accuracy of the classification model and the speed of the machine learning pipeline, a feature selection stage is introduced in the BCI application. Feature selection algorithms are categorized into two groups: filters and wrappers [25]. The categorizations depend on the metric employed to validate the feature or subset of features. For filters, that assessment is completed using specific criteria, for example, information

gain or redundancy, totally independent from the learning model. For wrappers, the evaluation criterion is the accuracy obtained by the learning model employing a specific subset of features.

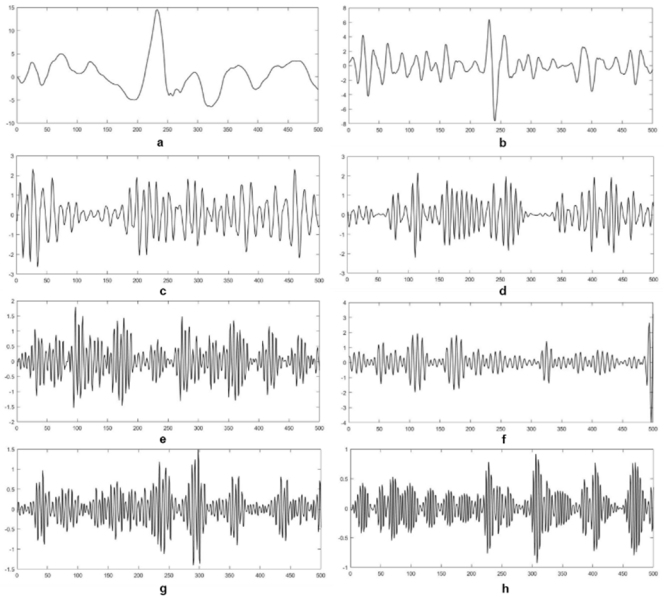

Fig. 2. Reconstructed signals for each sub-band of a sample MI EEG signal from channel C3: a) 0-4Hz, b) 4-8Hz, c) 8-12Hz, d) 12-16Hz, e) 16-20Hz, f) 20-24Hz, g) 24-28Hz, h) 28-32Hz

TABLE I. FEATURES FOR THE BCI MODEL

Feature	Reference	Number of features (for two EEG channels)
Mean of the absolute values of each sub-band	[26]	16
Average amplitude change of each sub-band	[27]	16
Standard deviation of each sub-band	[28]	16
Variance of each sub-band	[29]	16
Energy of each sub-band	[21]	16
Entropy of the coefficients of each sub-band	[28]	16
Phase Locking Values of each sub-band	[30]	8
Root mean square of each sub-band	[27]	16
Ratio of the energy of adjacent sub-bands		14

Specifically, in [18], after comparing several feature selection algorithms from filter and wrapper approaches, it was demonstrated that a GA as a wrapper approach produced a relevant subset of features that resulted in better classification accuracy from the learning model. Moreover, our work presented in [5] described a QiEA wrapper approach that outperformed the results of a classical GA with a significant improvement on convergence time for this specific BCI and EEG processing applications. Despite the advantages of this algorithm, the definition of the magnitude of the rotated angle had a great impact in both convergence speed and performance of the learning model. A new approach that can improve the former limitation is the addition of chaotic behavior to the QiEA by including variants of chaotic crossover operator and chaotic quantum update gate based on pseudorandom chaotic maps. The proposed binary CQiEA, from the extent our knowledge, has never been applied for feature selection, BCI or EEG signals processing.

1) Classical QiEA

In QiEAs with binary representation, Qubits are the basic processing units (as in any quantum computer). These elements have the particular property of a quantum system of being in a coherent superposition of states, managing to represent states $|0\rangle$, $|1\rangle$, and any superposition of both [31]. The state of a Qubit is described employing the expression:

$$|\psi\rangle = \alpha|0\rangle + \beta|1\rangle \quad (1)$$

where α and β are complex values known as probability amplitude for the system to take any of the states. Therefore, these values have to comply with the condition that $|\alpha|^2 + |\beta|^2 = 1$, where $|\alpha|^2$ and $|\beta|^2$ are the probabilities of observing states $|0\rangle$ or $|1\rangle$, respectively.

A set of consecutive Qubits defines a quantum chromosome, which, when observed, collapses to a classical individual. The general representation of a chromosome with m Qubits is shown in Equation 2.

$$q_j^t = \begin{bmatrix} \alpha_{j1}^t \\ \beta_{j1}^t \end{bmatrix} \begin{bmatrix} \alpha_{j2}^t \\ \beta_{j2}^t \end{bmatrix} \dots \begin{bmatrix} \alpha_{jm}^t \\ \beta_{jm}^t \end{bmatrix} \quad (2)$$

The quantum population $Q(t) = \{q_1^t, q_2^t, \dots, q_n^t\}$ is initialized by setting the probability amplitude of each Qubit to $(1/\sqrt{2})$ for both states, guaranteeing that at the beginning the probability of observing each state is equal. The crossover operator employed usually is the uniform crossover [32]. The main operator over the quantum population is the quantum rotating gates, which acts over probability amplitudes of Qubits, guiding the evolution process to the best solution in the population. This process is defined as Update:

$$\begin{bmatrix} \alpha_{ji}^{t+1} \\ \beta_{ji}^{t+1} \end{bmatrix} = \begin{bmatrix} cos\,\Delta\theta & -sin\,\Delta\theta \\ sin\,\Delta\theta & cos\,\Delta\theta \end{bmatrix} \begin{bmatrix} \alpha_{ji}^t \\ \beta_{ji}^t \end{bmatrix} \quad (3)$$

where $\Delta\theta$ is the rotated angle that controls the angular approximation of the Qubit state to $|0\rangle$ or $|1\rangle$. In this way, the selection of the right magnitude for this parameter is of vital importance for the performance of the algorithm. The evolution is terminated when the maximum number of generations is reached.

2) Chaotic Systems

Chaotic systems is a term that embodies phenomena that behaves as an irregular series of elements that are defined by a relatively simple rule [17]. Such systems are described as nonlinear and deterministic, and can be represented as maps (singular or multidimensional functions in which the value of

x_{n+1} is defined only by x_n). Other form of representing chaotic systems is through attractors, which are patterns formed when the system is represented in the phase space [33]. As main characteristics, chaotic systems are dynamical and present a great sensitivity to initial conditions and defined parameters. Consequently, small variation in these values can generate big differences in the system when iterations advance; ergodicity, and pseudorandom behavior [34].

3) Chaotic QiEA

Given the chaotic nature of Qubits, fast convergence rate and capacity of avoiding local minima [35], we propose to substitute the randomness in the QiEA by pseudo-random sequences known as chaotic maps. In this way, we introduce pattern-based ergodic disorderliness to the algorithmic structure that can improve the performance of the evolutionary process [15]. Two operators of the algorithm are affected by this change: the crossover operator and the quantum rotation gate.

Uniform crossover, in its standard form, swaps two parents' genes with a probability of 0.5. In [32] it was demonstrated that this probability (P_c) can be modified to decrease its disruption capacity. Therefore, the right value of this probability produces a right balance between exploration and exploitation. In our approach, this probability is not static, being defined by a chaotic sequence $\aleph$ (Equation 4).

$$P_c(t) = \aleph(t-1) \tag{4}$$

The second operator is the chaotic quantum rotation gate. In the classical QiEA, the value of $\Delta\theta$ can be maintained constant or defined by a lookup table, which increases the computational complexity of the algorithm. In the proposed CQiEA, this value is extracted from the chaotic map in that generation. Considering that the variations of this angle should be proportional to π and the outputs of chaotic maps can be limited to the unity range, then:

$$\Delta\theta(t) = \pi \cdot \aleph(t-1) \tag{5}$$

As chaotic systems are sensitive to the initial conditions, in the CQiEA, after generating the chaotic map, a random number determines the starting position of the system over the series. This approach produced different starting positions for each experiment and chaotic operator. Additionally, given that chaotic maps can be one or two-dimensional, for two-dimensional maps the method of folding the attractor around the y-axis [9] is used. This technique is formulated in Equation 6, in which the output value of the map $\aleph(t)$ is determined by the absolute value of the output of the map in the x axis over the maximum value of both generated chaotic series.

$$\aleph(t) = abs\big(\aleph_x(t)\big)/\max(\aleph_{x,y}(t)) \tag{6}$$

A flowchart of the CQiEA structure is shown in Fig. 3. To apply this algorithm for the feature selection stage in a BCI system, a Quantum chromosome has 134 Qubits (one Qubit for each feature), and each observation generates a classical individual that defines, depending on the binary value of each bit, which subset of features are selected to train the learning model. The fitness of each observation is determined by the accuracy of an MLP with 10 neurons in the hidden layer and training five models with random initialization of the weights. The neural network with the best classification accuracy is selected for the fitness value. A simplified diagram of the CQiEA and how it is employed for feature selection is shown in Fig. 4.

Six well known and commonly utilized chaotic maps including both one-dimensional and two-dimensional categories are employed to validate the quality of the approach and determine the best map for our specific application. Specifications of these maps are illustrated in Table II.

4) Classification

The classification stage is implemented employing an MLP with dynamic topology. In this model, the neurons of the hidden layer are varied between 5 and 20, and each network is trained 5 times in order to obtain the best possible accuracy. In BCI applications, this classifier is regarded as highly accurate and robust [16]. This network is different that the model employed inside the wrapper training, which has a fixed topology.

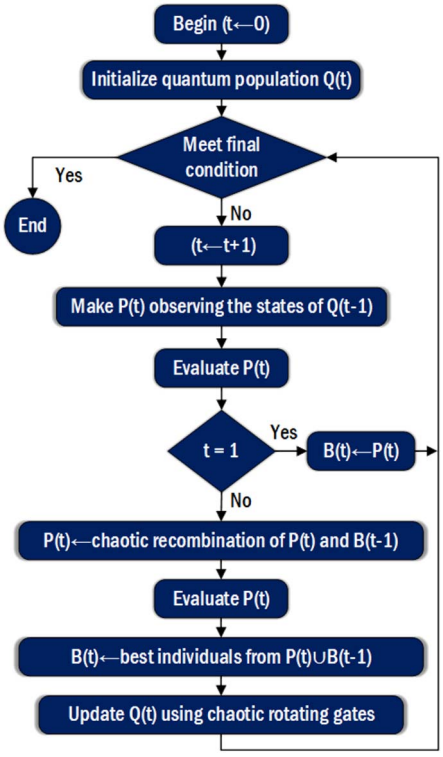

Fig. 3. Flowchart of CQiEA

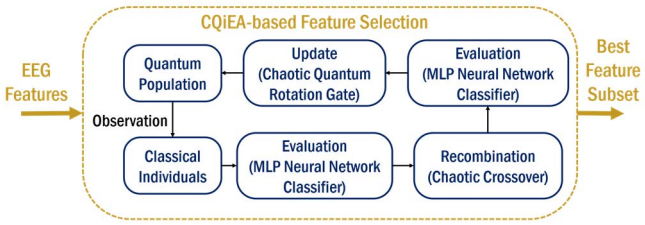

Fig. 4. Simplified diagram of the CQiEA for feature selection

TABLE II. DEFINITION OF CHAOTIC SYSTEMS EMPLOYED IN THIS WORK

Chaotic System	Definition	Parameters
Burgers map	$X_{n+1} = aX_n - {Y_n}^2$ $Y_{n+1} = bY_n + X_nY_n$	a = 0.75 b = 1.75
Henon map	$X_{n+1} = a - {X_n}^2 + bY_n$ $Y_{n+1} = X_n$	a = 1.4 b = 0.3
Ikeda map	$X_{n+1} = \gamma + \mu(X_n \cos\varphi + Y_n \sin\varphi)$ $Y_{n+1} = \mu(X_n \cos\varphi + Y_n \sin\varphi)$ $\varphi = \beta - \alpha/(1 + {X_n}^2 + {Y_n}^2)$	α = 6 β = 0.4 γ = 1 μ = 0.9
Logistic map	$X_{n+1} = aX_n(1 - X_n)$	a = 4
Quadratic map	$X_{n+1} = a - {X_n}^2$	a = 1.95
Tinkerbell map	$X_{n+1} = {X_n}^2 - {Y_n}^2 + aX_n + bY_n$ $Y_{n+1} = 2X_nY_n + cX_n + dY_n$	a = 0.9 b = -0.6 c = 2 d = 0.5

III. RESULTS AND DISCUSSION

The data employed in this work were provided by the BCI Competitions II (Dataset III-MI) and III (Dataset IIIb-MI), offered by the Department of Medical Informatics of the Institute for Biomedical Engineering of Graz University of Technology [36], [37]. The data contain EEG signals from three subjects that performed right and left hand MI tasks. The signals were filtered between 0.5 to 30Hz. Other details of the data are offered in Table III.

All models were developed using Matlab 2016a software tool. For the classification process, the dataset was normalized to a range of 0 to 1 and the training set divided into 70% trials for training and 30% for validation. The parametrization for the CQiEA algorithm was set as illustrated in Table IV, with values similar to the ones set for the QiEA in [5], in order to establish a direct comparison with those reported results.

TABLE III. CHARACTERISTICS OF THE DATA

Dataset	Subject	Trial Duration	Electrodes	Sampling Frequency	Training/ Test Samples
III-MI	A2	9s	C3 and C4	128Hz	140/140
IIIb-MI	S4	7s		125Hz	540/540
	X11				540/540

TABLE IV. PARAMETERS OF THE CQIEA

Parameter	Value
Number of quantum individuals	5
Number of observations	40 (8 observations for each quantum individual)
Number of Generations	40

The analysis of the results is twofold. Firstly, the characteristics of the evolutionary process for the three subjects are reported and discussed. Secondly, the results of the selected subset of features by the best models over the test set are analyzed.

Figs 5, 6, and 7 show the results of the selected chaotic maps for the three subjects, with the addition of the results of the QiEA presented in [5] and a classical GA over the validation set. Observing the figures, it is clear the significant convergence rate and the capacity of reaching the global optima of the proposed CQiEA. For subjects S4 and X11, Logistic and Ikeda maps resulted in a faster convergence when compared with the QiEA and the GA, obtaining higher values of accuracy in the evolutionary process. The number of evaluations needed to reach the maximum accuracy was reduced by 55% (from 968 to 440 evaluations) for Logistic Map and Subject S4 and around 39% (from 520 to 320 evaluations) for Ikeda map and Subject X11. Respectively, the maximum accuracy was improved by around 1% in S4 and 1.25% in X11.

In Fig. 7, the same behavior of the evolutionary process for subject A2 can be observed for Logistic and Tinkerbell sequences. This is a clear indication that, effectively, chaotic behavior enhances the performance of QiEAs, not only by reducing the number of evaluations needed to reach the maximum accuracy but also by increasing the value of that maximum accuracy.

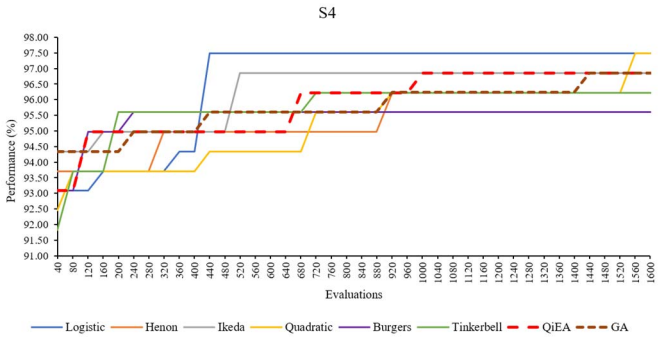

Fig. 5. Results from experiments with different chaotic maps for the proposed CQiEA, a classical QiEA and a GA for Subject S4

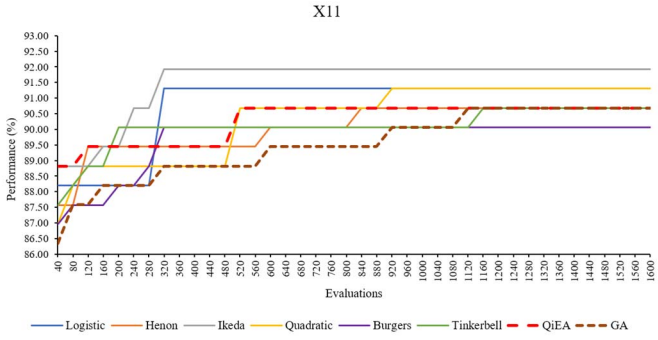

Fig. 6. Results from experiments with different chaotic maps for the proposed CQiEA, a classical QiEA and a GA for Subject X11

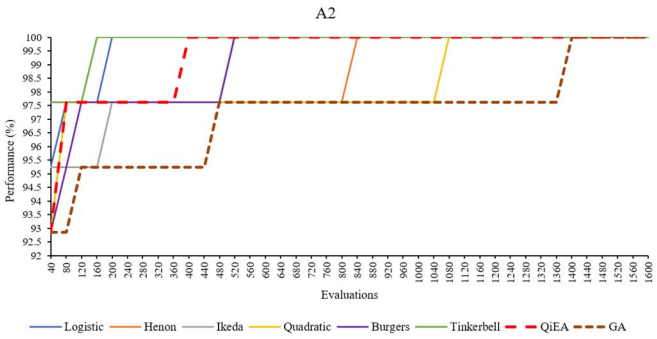

Fig. 7. Results from experiments with different chaotic maps for the proposed CQiEA, a classical QiEA and a GA for Subject A2

Of all chaotic maps tested, the one with better results was the Logistic map, followed by the Ikeda map. In general, for the three subjects, the Logistic map presented a significant improvement, being the second-best both on convergence time and maximum accuracy for subjects X11 and A2, and the best one in those indicators for S4. The Ikeda map presented outstanding results for X11, being the second-best for S4. However, for subject A2, the performance was limited, being surpassed in convergence rate even by the QiEA model. The quality of Logistic maps for the enhancement of QiEA is in agreement with conclusions reported in the literature [15].

The other chaotic maps included in the analysis presented a significant variation in their performance for different subjects. For S4 and X11, only the Quadratic map obtained an accuracy superior to the QiEA, but with a bigger convergence time. Exceptionally, the Tinkerbell map was the best for subject A2, showing poorer performances for the other subjects. Henon and Burgers maps did not present positive results, which seems that they are not suitable for this specific feature selection task in MI EEG signals classification.

The computational time of each evaluation is similar for each algorithm, given that they are configured with the same number of observations (therefore the same number of classical individuals), and each observation evaluates the same classifier. The introduction of chaotic operators in the CQiEA and the different number of features of each evaluation did not presented significant modifications to the computational time of the evaluations.

The mean accuracy and standard deviation of the results obtained when classifying the test set with the best subset of features recommended by ten runs of the CQiEA with Logistic map and Ikeda map, and of the classical GA and QiEA are presented in Table V. In general, test accuracies for the CQiEA approaches are lower than the values for the QiEA and GA. The cause of such results can be related to the nature of the wrapper approach, which, depending on the classifiers accuracies over a validation set, can suffer from overfitting, limiting in this way the generalization properties of the selected subset of features. The tradeoff then would be related to the selection of an algorithm with faster convergence time of the whole machine learning pipeline, losing a small amount of accuracy in new data, or to select another method more computationally costly. Moreover, with the significant improvement of the convergence time, other methods to avoid overfitting can be included, for example, it could be applied some alternative of cross-validation. The causes of this difference between the accuracies of the CQiEA and the other models will be investigated in further depth in future works.

Another way to validate if the difference between accuracies of Table V is significant is to apply a statistical validation. The Friedman test [38] was selected as statistical test, with the null hypothesis stating that all the algorithms are equivalent, presenting the same rank. The rejection of this hypothesis means that exist significant differences between the algorithms. The obtained Friedman approximation value (χ_F^2) is 3.4 for a number of tested algorithms of 4 and 3 subjects. For a $p<0.001$, the critical value indicated by the Table of Chi-Square Distribution [38] for a degree of freedom of k-1 was 16.27. As χ_F^2 is smaller than the critical value, then the null hypothesis cannot be rejected. Therefore, there not exist a statistically significant difference between the results of the applied feature selection models. Moreover, even for $p<0.1$, a critical value of 6.25 maintains the former conclusion.

The advantages of introducing chaotic systems to QiEAs is twofold. In the first place, by altering both crossover and quantum gates operators, the balance between exploration and exploitation is enhanced, allowing to search into new spaces. In the second place, the convergence speed is greatly improved, allowing the system to obtain solutions of better quality (e.g.: new values of maximum accuracies for subjects S4 and X11).

TABLE V. RESULTS OF THE BEST SUBSET OF FEATURES FOR THE BEST APPROACHES OF CQIEA, QIEA, AND GA

	S4		**X11**		**A2**	
	Mean Accuracy	Std	Mean Accuracy	Std	Mean Accuracy	Std
CQiEA - Logistic	87.88	0.98	81.96	0.95	95.43	1.30
CQiEA - Ikeda	89.27	1.47	82.52	0.76	94.71	0.64
QiEA	89.82	1.05	83.62	0.89	95.29	0.92
GA	89.84	0.98	83.74	0.74	95.00	0.78

IV. CONCLUSIONS

In this work, we have investigated the effects of adding ergodicity to a QiEA through the utilization of different chaotic sequences to produce variants of chaotic crossover operator and chaotic quantum update gate for feature selection applications on BCI based on MI EEG signals. Our hypothesis stated that, according to evidence of the advantages of the combination of chaotic systems and other evolutionary algorithms, the performance of the QiEA also can be improved by this technique. The main objective was, due to the need of individual training for each subject in BCI applications, to shorten the processing time of the wrapper approach, maintaining a good level of accuracy in the classification of user intention. The CQiEA was evaluated with data from three different subjects available at BCI Competitions and six

commonly used chaotic sequences, and the results were compared with the results of a QiEA and a GA (introduced in [5]). The quality of the algorithm and the feasibility of each chaotic map for this task were assessed employing an MLP as a classifier.

The proposed CQiEA demonstrated that, with an adequate chaotic map (Logistic or Ikeda), it can reach the maximum accuracy in much less time than both QiEA and classical GA. Additionally, when tested with new data, the algorithm presented a small decrease in the accuracy, which can be corrected by modifications of the learning model employed in the feature selection process (e.g.: inclusion of the method of cross-validation). The experiments implemented demonstrated that, for a greater convergence speed, CQiEA can be an effective algorithm for the feature selection stage in BCI applications. Particularly, even with a drop in the final classification accuracy, the results are very high and present a much shorter convergence time than QiEA and GA counterparts.

As future work, the causes of the limitation on the generalization capabilities of the model will be further investigated. In this sense, the algorithm can be enhanced by considering changes in the learning model that improve the final classification accuracy by tackling the possible overfitting of the MLP. Another interesting task can be the hybridization of this binary approach with a real representation [1], making a neuroevolutionary model that includes feature selection and the optimization of parameters of the learning model or/and preprocessing steps. Finally, the advantages of this algorithm for BCI applications can be evaluated in a real model, including online data obtained with an EEG headset and an orthosis for neurorehabilitation purposes.

REFERENCES

[1] A. V. A. da Cruz, M. M. B. R. Vellasco, and M. A. C. Pacheco, "Quantum-Inspired Evolutionary Algorithm for Numerical Optimization," in *Hybrid Evolutionary Algorithms*, A. Abraham, C. Grosan, and H. Ishibuchi, Eds. Berlin, Heidelberg: Springer Berlin Heidelberg, 2007, pp. 19–37.

[2] A. Manju and M. J. Nigam, "Applications of quantum inspired computational intelligence: A survey," *Artif. Intell. Rev.*, vol. 42, no. 1, pp. 79–156, 2014.

[3] G. Zhang, "Quantum-inspired evolutionary algorithms: a survey and empirical study," *J. Heuristics*, vol. 17, no. 3, pp. 303–351, Jun. 2011.

[4] R. González, M. Vellasco, and K. Figueiredo, "Resource optimization for elective surgical procedures using quantum-inspired genetic algorithms," in *Proceedings of the Genetic and Evolutionary Computation Conference on - GECCO '19*, 2019, pp. 777–786.

[5] A. C. Ramos and M. Vellasco, "Quantum-inspired Evolutionary Algorithm for Feature Selection in Motor Imagery EEG Classification," in *2018 IEEE Congress on Evolutionary Computation, CEC 2018 - Proceedings*, 2018.

[6] D. Szwarcman, D. Civitarese, and M. Vellasco, "Quantum-Inspired Neural Architecture Search," in *Proceedings of the International Joint Conference on Neural Networks*, 2019, vol. 2019-July.

[7] K. H. Han and J. H. Kim, "Quantum-inspired evolutionary algorithms with a new termination criterion, Hε gate, and two-phase scheme," *IEEE Trans. Evol. Comput.*, vol. 8, no. 2, pp. 156–169, Apr. 2004.

[8] H. Wang, J. Liu, J. Zhi, and C. Fu, "The improvement of quantum genetic algorithm and its application on function optimization," *Math. Probl. Eng.*, vol. 2013, no. 1, 2013.

[9] R. Senkerik, A. Viktorin, M. Pluhacek, and T. Kadavy, "On the Population Diversity for the Chaotic Differential Evolution," in *2018 IEEE Congress on Evolutionary Computation, CEC 2018 - Proceedings*, 2018.

[10] L. Y. Chuang, C. J. Hsiao, and C. H. Yang, "Chaotic particle swarm optimization for data clustering," *Expert Syst. Appl.*, vol. 38, no. 12, pp. 14555–14563, Nov. 2011.

[11] G. Fuertes, M. Vargas, M. Alfaro, R. Soto-Garrido, J. Sabattin, and M. A. Peralta, "Chaotic genetic algorithm and the effects of entropy in performance optimization," *Chaos*, vol. 29, no. 1, Jan. 2019.

[12] C. Hui, Z. Jiashu, and Z. Chao, "Chaos updating rotated gates quantum-inspired genetic algorithm," in *2004 International Conference on Communications, Circuits and Systems*, 2004, vol. 2, pp. 1108–1112.

[13] S. Zhao, G. Xu, T. Tao, and L. Liang, "Real-coded chaotic quantum-inspired genetic algorithm for training of fuzzy neural networks," *Comput. Math. with Appl.*, vol. 57, no. 11–12, pp. 2009–2015, Jun. 2009.

[14] S. Bhattacharyya and S. Dey, "An efficient quantum inspired genetic algorithm with chaotic map model based interference and fuzzy objective function for gray level image thresholding," in *Proceedings - 2011 International Conference on Computational Intelligence and Communication Systems, CICN 2011*, 2011, pp. 121–125.

[15] A. Mozaffari, M. Emami, N. L. Azad, and A. Fathi, "Comparisons of several variants of continuous quantum-inspired evolutionary algorithms," *J. Exp. Theor. Artif. Intell.*, vol. 29, no. 4, pp. 869–909, Jul. 2017.

[16] F. Lotte *et al.*, "A review of classification algorithms for EEG-based brain-computer interfaces: A 10 year update," *Journal of Neural Engineering*, vol. 15, no. 3. Institute of Physics Publishing, 16-Apr-2018.

[17] H. Nagashima, Y. Baba, and M. Nakahara, *Introduction to Chaos*, 1st ed. CRC Press, 1999.

[18] A. Celecia, R. Gonzalez, and M. Vellasco, "Feature Selection methods applied to Motor Imagery task classification," in *2016 IEEE Latin American Conference on Computational Intelligence (LA-CCI)*, 2016, pp. 1–6.

[19] A. Celecia, R. Gonzalez, M. Vellasco, and P. Vellasco, "Ensemble of classifiers applied to motor imagery task classification for BCI applications," in *2017 International Joint Conference on Neural Networks (IJCNN)*, 2017, pp. 2995–3002.

[20] B. Graimann, B. Allison, and G. Pfurtscheller, "Brain–Computer Interfaces: A Gentle Introduction," in *Brain-Computer Interfaces*,

Springer Berlin Heidelberg, 2009, pp. 1–27.

[21] W. Ting, Y. Guo-zheng, Y. Bang-hua, and S. Hong, “EEG feature extraction based on wavelet packet decomposition for brain computer interface,” *Measurement*, vol. 41, no. 6, pp. 618–625, 2008.

[22] K. K. Ang *et al.*, “A Large Clinical Study on the Ability of Stroke Patients to Use an EEG-Based Motor Imagery Brain-Computer Interface,” *Clin. EEG Neurosci.*, vol. 42, no. 4, pp. 253–258, 2011.

[23] W. Yi *et al.*, “EEG oscillatory patterns and classification of sequential compound limb motor imagery,” *J. Neuroeng. Rehabil.*, vol. 13, no. 1, p. 11, 2016.

[24] A. Subasi and M. Ismail Gursoy, “EEG signal classification using PCA, ICA, LDA and support vector machines,” *Expert Syst. Appl.*, vol. 37, no. 12, pp. 8659–8666, 2010.

[25] H. Liu, H. Motoda, R. Setiono, and Z. Zhao, “Feature Selection : An Ever Evolving Frontier in Data Mining,” *J. Mach. Learn. Res. Work. Conf. Proc. 10 Fourth Work. Featur. Sel. Data Min.*, pp. 4–13, 2010.

[26] S.-H. Lee and J. S. Lim, “Minimum feature selection for epileptic seizure classification using wavelet-based feature extraction and a fuzzy neural network,” *Appl. Math. Inf. Sci.*, vol. 8, no. 3, pp. 1295–1300, 2014.

[27] M. H. Alomari, E. A. Awada, A. Samaha, and K. Alkamha, “Wavelet-Based Feature Extraction for the Analysis of EEG Signals Associated with Imagined Fists and Feet Movements,” *Comput. Inf. Sci.*, vol. 7, no. 2, p. 17, Mar. 2014.

[28] R. K. Chaurasiya, N. D. Londhe, and S. Ghosh, “Statistical Wavelet Features, PCA, and SVM Based Approach for EEG Signals Classification,” *World Acad. Sci. Eng. Technol. Int. J. Electr. Comput. Energ. Electron. Commun. Eng.*, vol. 9, no. 2, pp. 182–186, 2015.

[29] L. Vega-Escobar, A. E. Castro-Ospina, and L. Duque-Muñoz, “Feature extraction schemes for BCI systems,” in *2015 20th Symposium on Signal Processing, Images and Computer Vision, STSIVA 2015 - Conference Proceedings*, 2015, no. 76.

[30] W.-Y. Hsu, “Wavelet-Coherence Feaures for Motor Imagery EEG Analysis Posterior to EOG Noise Elimination,” *Int. J. Innov. Comput. Inf. Control*, vol. 9, no. 2, pp. 465–475, 2013.

[31] Kuk-Hyun Han and Jong-Hwan Kim, “Quantum-inspired evolutionary algorithm for a class of combinatorial optimization,” *IEEE Trans. Evol. Comput.*, vol. 6, no. 6, pp. 580–593, Dec. 2002.

[32] W. M. Spears and K. a. De Jong, “On the Virtues of Parameterized Uniform Crossover,” *Proc. Fourth Int. Conf. Genet. Algorithms*, pp. 230–236, 1991.

[33] K. Mohanchandra, S. Saha, and A. T. Azar, “Evidence of chaos in EEG signals: An application to BCI,” in *Studies in Fuzziness and Soft Computing*, vol. 337, Springer Verlag, 2016, pp. 609–625.

[34] G. I. Sayed, A. E. Hassanien, and A. T. Azar, “Feature selection via a novel chaotic crow search algorithm,” *Neural Comput. Appl.*, vol. 31, no. 1, pp. 171–188, Jan. 2019.

[35] H. Lu, X. Wang, Z. Fei, and M. Qiu, “The effects of using chaotic map on improving the performance of multiobjective evolutionary algorithms,” *Math. Probl. Eng.*, vol. 2014, 2014.

[36] A. Schlögl, “Data set: BCI-experiment.” BCI competition 2003, 2002.

[37] A. Schlögl, “Dataset IIIb: Non-stationary 2-class BCI data.” BCI Competition III, 2005.

[38] D. J. Sheskin, *Handbook of Parametric and Nonparametric Statistical Procedures: Second Edition*. Boca Raton, Florida: Chapman & Hall, 2000.